International Journal of Engineering, Management, Humanities and Social Sciences Paradigms (Volume 30, Special Issue of Nov 2018)
ISSN (Online): 2347-601X and Website: www.ijemhs.com

Concrete-Bonded FRP and Steel Plate Anchorage Strength Models

[1*]Suchismita Mallik, [2]Archana Anand
[1*] Asst. Professor, Dept. Of Civil Engineering, NIT BBSR,
[2]Asst. Professor Dept. of Civil Engineering, HIT, BBSR
[1*]malliksuchismita1992@gmail.com, anandarchana188@gmail.com

ABSTRACT: Since the 1960s, weak reinforced-concrete structures have been reinforced via external bonding of steel plates. Due to their superior qualities, fiber-reinforced polymer (FRP) plates have replaced steel plates in recent years. The end anchorage strength is a crucial consideration in the design of a successful retrofitting solution using externally joined plates. This study initially reviews the available anchorage strength models for shear-bonded junctions between FRP and concrete as well as steel and concrete. The shortcomings of all current models are then revealed once these models are evaluated using experimental data gathered from the literature. Ultimately, a fresh, straightforward, and logical model is put out in light of recent fracture mechanics research and experimental findings. This novel model accurately predicts the effective bond length and closely fits experimental measurements of bond strength. The new model is thus suited for actual use in the design of bonded joints between FRP and concrete as well as steel and concrete.

INTRODUCTION

Since the 1960s, weak reinforced-concrete (RC) structures have been reinforced via external bonding of steel plates. Due to their superior qualities, fiber-reinforced polymer (FRP) plates have been employed to replace steel plates more and more recently. The end anchorage strength is a crucial factor in the design of an efficient retrofitting solution employing externally bonded plates, and extensive study has been done on this problem. This study looks at anchorage failure caused by cracks that spread parallel to bonded plates near or along the adhesive/concrete interface, commencing from the critically stressed point and moving towards the anchored end of the plate. For plates or strips bonded to the sidewalls of beams for shear strengthening, this is the typical anchorage failure mode (Teng et al. 2000). It is also one of the potential failure modes in reinforced concrete slabs (RC) and beams strengthened with bonded soffit plates and strips when debonding originates at a significant crack that extends away from but towards the plate end (Teng et al. 2000; Smith et al. 2001Due to the load concentration at the plate end, another significant anchorage failure mode for a beam with a bonded soffit plate begins there. The latter is not included in the current paper; for more information, refer to other sources of data (Zhang et al. 1997; Malek et al. 1998; Teng et al. 2000). It is important to emphasise the differences between these two failure modes; the failure mode discussed in this work is known as shear anchorage failure or shear debonding failure. Substantial experimental and theoretical work exists on shear anchorage strength. Experiments have been carried out using several setups, including single shear tests (Chajes et al. 1995, 1996; Bizindavyi and Neale 1997, 1999; Täljsten 1997), double shear tests (van Gemert 1980; Swamy et al. 1986; Ko- batake et al. 1993; *FORCA* 1994; Brosens and van Gemert 1997; Fukuzawa et al. 1997; Hiroyuki and Wu 1997; Maedaet al. 1997; Neubauer and Rostásy 1997), and modified beam tests (van Gemert 1980; Ziraba et al. 1995). Theoretical work has included both fracture mechanics analysis (Triantafillouand Plevris 1992; Holzenkämpfer 1994; Täljsten 1994; Yuan and Wu 1999; Yuan et al. 2001) and the development of em- pirical models based on regression of experimental data and/ or simplistic assumptions (van Gemert 1980; Chaallal et al. 1998; Khalifa et al. 1998).

This paper first presents a review of anchorage behavior under single/double shear tests (Fig. 1) and available shear anchorage strength models in the literature. These models are then assessed with experimental data collected from the liter- ature, revealing the deficiencies of all existing models. Finally, a new simple, rational, and accurate design model is proposed based on an existing fracture mechanics analysis and experi- mental observations.

FAILURE MODES

For single or double shear tests, there are six possible dis- tinct failure modes in theory for an FRP or steel plate bonded to concrete, although they may be mixed in an actual failure. These are listed below in the order of their likeliness, based on existing test data collected in Table 1.

1. Concrete failure
2. Plate tensile failure including FRP rupture or steel yield-ing
3. Adhesive failure
4. FRP delamination for FRP-to-concrete joints
5. Concrete-to-adhesive interfacial failure
6. Plate-to-adhesive interfacial failure

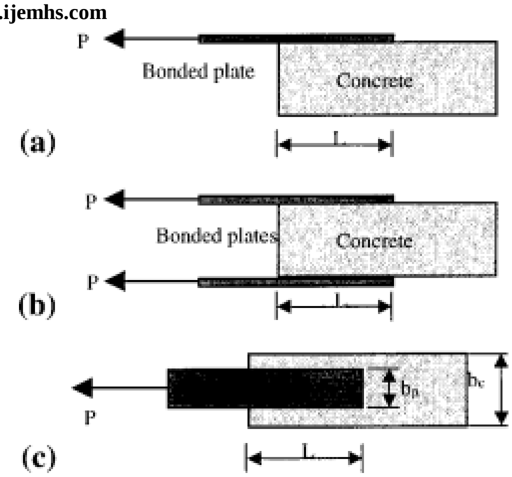

FIG. 1. Single and Double Shear Tests: (a) Single Shear Test; (b) Dou- ble Shear Test; (c) Plan

TABLE 1. Single and Double Shear Test Data Collected from Literature[a]

		Concrete					Plate							
Specimen reference number[b,c]	Adhesive E_a (MPa)	Width b_c (mm)	Thickness t_c (mm)	Compressive strength f'_c (MPa)	Young's modulus E_c (MPa)	Tensile strength f_{ct} (MPa)	Type	Thickness t_p (mm)	Width B_p (mm)	Bond length L (mm)	Young's modulus E_p (MPa)	Ultimate strength f_{up} (MPa)	Measured failure load P_u (N)	Failure mode[d]
BN1	3,304	150	150	42.5	33,500	3.50	GFRP	1	25.4	180	29,200	472	11,410	FR
BN2	3,304	150	150	42.5	33,500	3.50	GFRP	2	25.4	320	29,200	472	21,400	FR
BN3	3,257	150	150	42.5	33,500	3.50	CFRP	0.33	25.4	160	75,700	1,014	8,500	FR
BN4	3,257	150	150	42.5	33,500	3.50	CFRP	0.66	25.4	320	75,700	1,014	15,100	FR
C1	5,172	228.6	152.4	36.1	—	—	GFRP	1.016	25.4	76.2	108,478	1,655	8,462	CF
C2	5,172	228.6	152.4	47.1	—	—	GFRP	1.016	25.4	76.2	108,478	1,655	9,931	CF
C3	5,172	228.6	152.4	47.1	—	—	GFRP	1.016	25.4	76.2	108,478	1,655	10,638	CF
C4	5,172	228.6	152.4	47.1	—	—	GFRP	1.016	25.4	76.2	108,478	1,655	10,638	CF
C5	2,207	228.6	152.4	43.6	—	—	GFRP	1.016	25.4	76.2	108,478	1,655	10,531	CF
C6	234	228.6	152.4	43.6	—	—	GFRP	1.016	25.4	76.2	108,478	1,655	8,956	AF
C7	234	228.6	152.4	43.6	—	—	GFRP	1.016	25.4	76.2	108,478	1,655	9,610	CF
C8	1,584	228.6	152.4	43.6	—	—	GFRP	1.016	25.4	76.2	108,478	1,655	10,518	CF
C9	1,584	228.6	152.4	43.6	—	—	GFRP	1.016	25.4	76.2	108,478	1,655	11,199	CF
C10	1,584	228.6	152.4	24.0	—	—	GFRP	1.016	25.4	76.2	108,478	1,655	9,869	CF
C11	1,584	228.6	152.4	28.9	—	—	GFRP	1.016	25.4	76.2	108,478	1,655	9,343	CF
C12	1,584	228.6	152.4	43.7	—	—	GFRP	1.016	25.4	76.2	108,478	1,655	11,204	CF
C13	1,584	228.6	152.4	36.4	—	—	GFRP	1.016	25.4	50.8	108,478	1,655	8,094	CF
C14	1,584	228.6	152.4	36.4	—	—	GFRP	1.016	25.4	101.6	108,478	1,655	12,811	CF
C15	1,584	152.4	152.4	36.4	—	—	GFRP	1.016	25.4	152.4	108,478	1,655	11,917	CF
C16	1,584	152.4	152.4	36.4	—	—	GFRP	1.016	25.4	203.2	108,478	1,655	11,570	CF
M1	5,000	100	100	40.8	—	—	CFS	0.11	50	75	230,000	3,500	5,800	FD
M2	5,000	100	100	40.8	—	—	CFS	0.11	50	150	230,000	3,500	9,200	FD
M3	5,000	100	100	43.3	—	—	CFS	0.11	50	300	230,000	3,500	11,950	FD
M4	5,000	100	100	42.4	—	—	CFS	0.165	50	75	380,000	3,000	10,000	CF
M5	5,000	100	100	42.4	—	—	CFS	0.165	50	150	380,000	3,000	7,300	FR
M6	5,000	100	100	42.7	—	—	CFS	0.22	50	65	230,000	3,500	9,550	CF
M7	5,000	100	100	42.7	—	—	CFS	0.22	50	150	230,000	3,500	16,250	FD
M8	5,000	100	100	44.7	—	—	CFS	0.11	50	700	230,000	3,500	10,000	FD
C100 50A	6,700	200	200	—	35,000	3.90	CFRP	1.25	50	100	170,000	2,497	17,300	CF
C200 50A	6,700	200	200	—	35,000	4.10	CFRP	1.25	50	200	170,000	2,497	27,500	CF
C300 50A	6,700	200	200	—	35,000	4.30	CFRP	1.25	50	300	170,000	2,497	35,100	CF
C400 50A	6,700	200	200	—	35,000	4.30	CFRP	1.25	50	400	170,000	2,497	26,900	CF
S100 40A	6,700	200	200	—	35,000	4.20	Steel	2.9	40	100	205,000	399	21,100	CF
S200 40A	6,700	200	200	—	35,000	3.90	Steel	2.9	40	200	205,000	399	39,500	CF
S400 40A	6,700	200	200	—	35,000	4.30	Steel	2.9	40	400	205,000	399	41,100	CF
S50 60A	6,700	200	200	—	35,000	4.20	Steel	2.9	60	50	205,000	403	12,700	CF
S100 60A	6,700	200	200	—	35,000	4.10	Steel	2.9	60	100	205,000	399	20,000	CF
S150 60A	6,700	200	200	—	35,000	4.30	Steel	2.9	60	150	205,000	403	46,300	CF
S200 60B	6,700	200	200	—	35,000	4.10	Steel	2.9	60	200	205,000	399	48,800	CF
S400 60A	6,700	200	200	—	35,000	4.30	Steel	2.9	60	400	205,000	403	58,400	CF
S400 60B	6,700	200	200	—	35,000	4.10	Steel	2.9	60	400	205,000	399	53,000	CF
S100 80C	6,700	200	200	—	35,000	4.40	Steel	2.9	80	100	205,000	403	39,600	CF
S150 80A	6,700	200	200	—	35,000	3.90	Steel	2.9	80	150	205,000	403	50,900	CF
S200 80A	6,700	200	200	—	35,000	4.30	Steel	2.9	80	200	205,000	403	67,300	CF
S300 80C	6,700	200	200	—	35,000	4.10	Steel	2.9	80	300	205,000	403	68,000	CF
S500 80C	6,700	200	200	—	35,000	4.40	Steel	2.9	80	500	205,000	399	67,300	CF
S600 80B	6,700	200	200	—	35,000	4.10	Steel	2.9	80	600	205,000	403	71,400	CF
S800 80A	6,700	200	200	—	35,000	4.10	Steel	2.9	80	800	205,000	403	61,600	CF
S1	430–2,000	60	60	19.8	—	—	Steel	3	60	150	200,000	365–400	19,530	CF
S2	430–2,000	60	60	35.5	—	—	Steel	3	60	150	200,000	365–400	22,680	CF
S3	430–2,000	60	60	47.6	—	—	Steel	3	60	150	200,000	365–400	24,930	CF
S4	430–2,000	60	60	56.3	—	—	Steel	3	60	150	200,000	365–400	29,970	CF
S5	430–2,000	60	60	35.6	—	—	Steel	3	60	150	200,000	365–400	21,780	CF
S6	430–2,000	60	60	35.6	—	—	Steel	3	60	150	200,000	365–400	21,420	CF
S7	430–2,000	60	60	35.6	—	—	Steel	3	60	150	200,000	365–400	25,470	CF

[a]Young's modulus E_c, splitting tensile strength f_{ct} and cylinder compressive strength f'_c for concrete, and shear modulus G_a for adhesive were evaluated using the following relationships if they were not given in the original literature: $E_c = 4{,}730\sqrt{f'_c}$ MPa (ACI 318-89); $f_{ct} = 0.53\sqrt{f'_c}$ MPa (ACI 318-89); $f'_c = 0.79 f_c$ (BSI 8110, 1985); $G_a = E_a / 2(1 + \nu_a)$, $E_a = 5$ GPa, $\nu_a = 0.3$, and $t_a = 1$ mm are assumed if they were not given in the original literature.

[b]Some of the specimen reference numbers are assigned by the current writers because they were not available in the original paper.

[c]Specimens BN1–BN4 are from Bizindavyi and Neale (1999). Specimens A1–A5 and B1–B5 are from Brosens and van Gemert (1997). Specimens C1–C16 are from Chajes et al. (1996). Specimens M1–M8 are from Maeda et al. (1997). Specimens C100–C400 and S100–S800 are from Täljsten (1997). Specimens S1–S7 are from Swamy et al. (1986).

[d]Failure mode: FR = FRP rupture, CF = concrete fracture, FD = FRP delamination, AF = cohesive failure through adhesive.

The single and double shear test data shown in Table 1 have been collected from the existing literature based on an exten- sive literature survey; tests that were not sufficiently well doc- umented for analysis and interpretation have been excluded here. These data show that most experimental joints failed in the concrete a few millimeters beneath the concrete/adhesive interface (van Gemert 1980; Maeda et al. 1997). Interfacial failure, between either the adhesive and the concrete or the adhesive and the plate, is not found in Table 1. This is a con- sequence of the availability of strong adhesives that bond well to steel, FRP, and concrete. For the same reason, adhesive failure is rare, as only one such case is seen in Table 1. A

small number of specimens failed by FRP rupture and an equal number of specimens failed by FRP delamination. This paper is primarily concerned with concrete failure beneath the plate- to-concrete interface. Neubauer and Rostásy (1997) showed that the same energy release rate model is applicable to both the concrete fracture failure mode and the FRP delamination failure mode. This is because, even in the FRP delamination failure mode, concrete failure usually occurs in the first 20 –50% of the bond length, which is the key failure process and predominates the fracture energy release rate. Cracking then extends into the FRP matrix, leading to FRP delamination. Therefore, the new bond strength model developed in this pa-

per may also be applicable to FRP delamination failures. Plate tensile failure and pure adhesive-to-concrete interfacial failure are not included in this paper, as the former is governed by the properties of the bonded plate rather than the bonded joint, while the latter can be avoided by careful surface preparation.

EFFECTIVE BOND LENGTH

The tension in the plate is transferred to the concrete mainly via shear stresses in the adhesive in a short length nearest to the applied load. Van Gemert (1980) examined the stresses in steel plates bonded to a rectangular plain concrete prism in a double shear test. The tensile force in the steel plate was found to decay exponentially toward the anchored end of the plate. At higher loads, the distribution of the tensile force became more and more even in the initial bond zone. This means that practically no force was transferred from the plate to the con- crete in this zone, because the cracking of the concrete near the applied load shifted the active bond zone to new areas farther away from the loading point. This phenomenon has been confirmed by many other studies on steel-to-concretebonded joints (Täljsten 1997) and FRP-to-concrete bonded joints (Maeda et al. 1997).

The shift of the active bond zone means that at any onetime, only part of the bond is effective. That is, as cracking in the concrete propagates, bond resistance is gradually lost in the zone near the load, but in the meantime it is activated farther away from the load. The implication is, then, that the anchorage strength cannot always increase with an increase in the bond length, and that the ultimate tensile strength of a plate may never be reached, however long the bond length is. This leads to the important concept of effective bond length, be- yond which any increase in the bond length cannot increase the anchorage strength, as confirmed by many experimental studies (Chajes et al. 1996; Maeda et al. 1997; Täljsten 1997) and fracture mechanics analyses (Holzenkämpfer 1994; Yuan and Wu 1999; Yuan et al. 2001). However, a longer bond length may improve the ductility of the failure process.

This phenomenon is believed to be the primary reason for the observed low stresses in bonded plates at anchorage failure (Fig. 2). The ultimate stress in FRP at failure σ_{fu} has an av- erage value of 28% of the ultimate tensile strength f_{fu}, with a coefficient of variation (COV) of 40% (Fig. 2). This ratio is substantially higher for steel-to-concrete joints, with an aver- age value of σ_{su} / f_{su} = 58%, but the degree of scatter is similar (COV = 37%). The corresponding ratio to steel yielding stress is σ_{su} / f_{sy} = 71%. This phenomenon is substantially different from the bond behavior of internal reinforcement, for which a

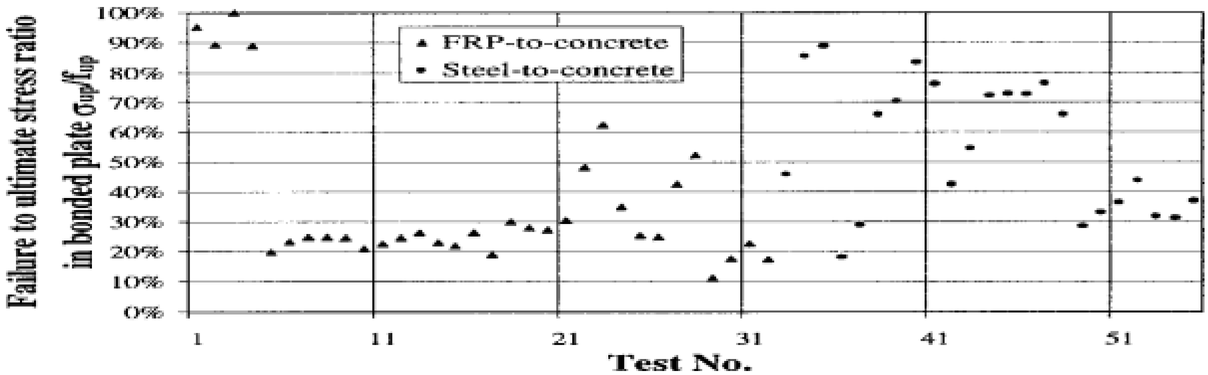

FIG. 2. Maximum Plate Stress at Bond Failure

$$r_u = 5.88L^{-0.669} \text{ (MPa)} \quad (1)$$

Tanaka (1996) presented another simple expression (Sato et al. 1996)

$$r_u = 6.13 - \ln L \text{ (MPa)} \quad (2)$$

where L is in millimeters. The ultimate bond strength of the joint P_u is given by multiplying r_u by the width b_p and length L of the bond area in the above two models.

Maeda et al. (1997) developed a more robust model that considers the effective bond length

$$r_u = 110.2 \times 10^{-6} E_p t_p \text{ (MPa)} \quad (3a)$$

where t_p (mm) and E_p (MPa) = thickness and Young's modulusof the bonded plate, respectively.

The ultimate bond strength P_u is obtained by multiplying r_u by the effective bond area $L_e b_p$. Here, the effective bond length L_e is given by

$$L_e = e^{6.13-0.580 \ln E_p t_p} \text{ (mm)} \quad (3b)$$

Note that E_p is in gigapascals and t_p is in millimeters in (3b). This model is obviously invalid if $L < L_e$.

Fracture Mechanics Based Models

Holzenkämpfer (1994) investigated the bond strength be- tween a steel plate and concrete using nonlinear fracture me- chanics (NLFM). The modified form by Niedermeier (1996; Blaschko et al. 1996) calculates the bond strength by using

bond length can always be designed for its full tensile strengthif there is sufficient concrete cover. This key aspect must be accounted for in the development of shear anchorage strength

Both FRP and Steel-To-Concrete

Source	Average	SD	COV	Average	SD	COV	Average	SD	COV
Hiroyuki and Wu (1997) (1)	2.87	0.95	33%	3.85	1.18	31%	3.24	1.09	34%
Tanaka (1996) (2)	2.92	1.65	56%	5.51	5.30	96%	4.02	3.96	99%
van Gemert (1980) (10)	2.19	1.12	51%	1.64	0.57	35%	1.91	0.96	50%
Chaallal et al. (1998) (11)	1.81	0.89	49%	1.68	0.70	42%	1.71	0.79	46%
Khalifa et al. (1998) (12)	1.07	0.24	23%	0.76	0.26	34%	0.93	0.29	31%
Neubauer and Rostásy (1997) (9)	0.82	0.15	18%	0.65	0.09	13%	0.74	0.15	20%
(16)	1.05	0.18	17%	0.94	0.11	12%	1.00	0.16	16%

Note: SD = standard deviation; COV = coefficient of variation.

the FRP plate. Because (11*b*) was based on limited experimental data and does not relate to the strength of concrete, its applicability is seriously limited. Another drawback of this proposal is that the effective bond length is not considered.

Khalifa et al. (1998) proposed a modification of Maeda et al.'s (1997) model [(3)] and included the effect of concrete strength, so that it could be used for design. They used the relationship that the bond strength between the FRP sheet and the concrete surface is a function of $(f_c')^{2/3}$ (Horiguchi and Saeki 1997). Because the concrete strength was 42 MPa in the experiments carried out by Maeda et al. (1997), the modified equation is thus

$$f_{ct} = 0.53\sqrt{f_c'} \text{ (MPa)} \quad (13)$$

Table 2 shows that, on average, the experimental observa- tion is 0.82 of that predicted by the model of Neubauer and Rostásy (1997) for FRPs [i.e., predictions are (1 − 0.82)/0.82 = 22% higher than observations, on average]. For steel plates, the average test-to-predicted strength ratio is 0.74 (i.e., pre- dictions are 55% higher than test observations). For the whole data set including both FRP and steel plates, the predictions of their model are 35% higher than experimental observations, on average. Another drawback of this model is the use of concrete surface tensile strength, which requires special tests, while concrete compressive strength is readily available in most cases.

—

c

PRACTICAL ENGINEERING MODEL

The effective bond length is calculated using (3*b*).

Neubauer and Rostásy (1997) proposed to use 75% of the ultimate bond strength for design, i.e., to reduce the factor of 0.64 in (9*a*) to 0.5.

Comparison with Experimental Observations

Table 2 compares the performance of some of the above models in predicting the experimental bond strengths given in Table 1 (27 FRP and 23 steel bond tests after excluding those failing by FRP rupture). Purely fracture mechanics based mod- els are not included in this comparison because the fracture energy and the shear-slip parameters are not available.

New Model

The shortcomings of the above models necessitate the de- velopment of a new model for practical design that is simple to use, rationally based, and capable of capturing the funda- mental features of the bond behavior and predicting the bond strength and the effective bond length with good accuracy.

For FRP-to-concrete bonded joints, the typical slip values are δ_1 = 0.02 mm and δ_f = 0.2 mm; i.e., δ_1 is small compared to δ_f. Therefore, the linearly decreasing shear-slip model [Fig. 2(b)] may be used. The NLFM solution for this case is (Yuan and Wu 1999).

experimental data statistically. They hugely underestimate the bond strength and, more important, lead to a very large scatter.

The chief cause for the poor performance may be that the effective bond length is not considered in these models. The models by Khalifa et al. (1998) and Neubauer and Rostásy *e*

e

(1997) from the regression of test data of FRP-to-concrete joints. As a result, it agrees reasonably well with experimental data for FRP-to-concrete joints, but not so well for steel-to- concrete joints. The chief drawback of this model is that it may greatly overestimate the shear stress at failure and un- derestimate the effective bond length. For example, (12) pre- dicts an average shear stress at failure of about 60 MPa and (3*b*) predicts an effective bond length of about 11 mm for the set of steel-to-concrete joints reported by Täljsten (1997), compared with an observed effective bond length of about 300 mm. It thus cannot be used for safe practical design.

Concrete surface tensile strength f_{ctm} was used in the model proposed by Holzenkämpfer (1994) and that proposed by Neu- bauer and Rostásy (1997). Because this strength is not avail- able for all of the data examined here (Table 1), the concrete splitting tensile strength f_{ct} is used instead here and it is esti- mated, if not given in the original source, from f_c' (MPa) using (MacGregor 1988)

The shear-slip properties in (14) may be expressed in terms of the concrete strength. The ultimate bond strength has been related to the concrete surface tensile strength [(4), (8), and (10)] and shear strength [(12)]. However, various experimental observations (Chajes et al. 1996) showed that the ultimate bond strength is proportional to $\sqrt{f_c'}$, similar to the bond strength of internal steel (British 1985) and FRP (Ehsani et al. 1996) reinforcement. This is confirmed by a regression anal- ysis of the test data in Table 1.

The coefficient α_Y in (14) [compared to (6)] appears to be very small for practical configurations compared to unity (varying from 0.001 to 0.034 for all of the tests in Table 1 except for the last seven specimens, which vary from 0.3 to 0.5). This term has arisen from the assumption that the stress distribution is uniform across the whole cross section of the concrete, as well as in the bonded plate. Because of localized bond behavior, this assumption is clearly invalid for the con-

crete. Instead, the width ratio of the bonded plate to the con- crete member b_p/b_c is shown to have a significant effect on the ultimate bond strength, in a form similar to the coefficient proposed by Holzenkämpfer (1994) [compared to (4*d*)]. If the

where

$$P_u = 0.427\beta_p\beta_L\sqrt{f_c'}b_pL_e$$

$$\Bigg] \frac{E\ t}{}$$

(16*a*)

width of the bonded plate is smaller than that of the concrete member, the force transfer from the plate to the concrete leadsto a nonuniform stress distribution across the width of the concrete member. A smaller b_p compared to b_c may result in a higher shear stress in the adhesive at failure, attributed to

L_e

e

the contribution from the concrete outside the bond area. The

regression of the test data of Table 1 (Fig. 4) shows that the

(16*c*)

ause it uses the cylinder concrete compressive strength f_c',

c

which is available in most cases. To compare this new model

By taking into account the above considerations, a simple ultimate bond strength model may be proposed based on (14) and the regression of test data in Table 1

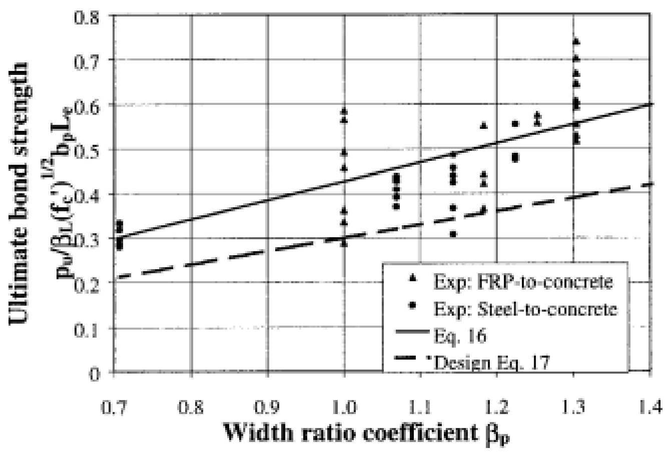

FIG. 4. Effect of Bonded Plate to Concrete Width Ratio on UltimateBond Strength

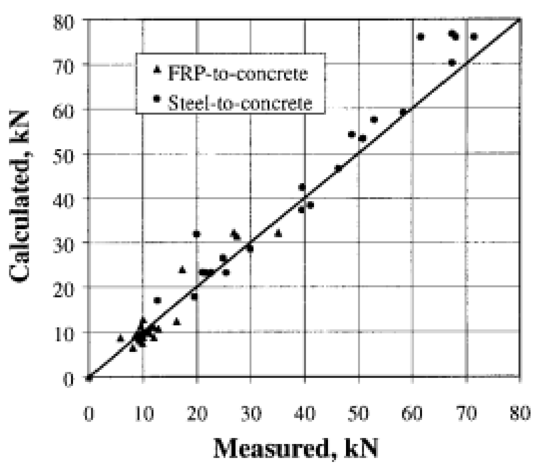

FIG. 5. Measured Values Via Calculated Bond Strength

with the experimental data in Table 1, the concrete split tensilestrength f_{ct} for the set of data presented by Täljsten (1997) needs to be converted to f_c'. This was done by first calculating f_c' from f_{ct} for each specimen using (13) and then scaling the results by multiplying all of the f_c' values obtained from f_{ct} by a single factor so that the average Young's modulus E_c found by using the American Concrete Institute (1989) relationship $E_c = 5{,}730\sqrt{f_c'}$ is 3.5 GPa, as given by Täljsten (1997). Both E_c and f_{ct} were used in this process in an attempt to find the actual f_c', because both are affected by many other factors apart from f_c'.

Table 2 shows that (16) agrees well with the test data for both FRP-to-concrete and steel-to-concrete bonded joints. Theratio of the observed to the predicted ultimate bond strength for the two types of joints has an overall average value of 1.00 and a corresponding standard deviation of 0.159 (Fig. 5).

Eq. (16*b*) shows that L_e increases linearly with $\sqrt{E_p t_p}$. The predicted values by the proposed new model for the effective bond length are in a close agreement with the very limited experimental observations (Table 3). A comparison in Fig. 6 shows that the empirical model proposed by Maeda et al.(1997) predicted the wrong trend on the effect of $E_p t_p$ on the effective bond length. Fig. 7 shows the effect of bond lengthon the ultimate bond strength. The experimental data are nicely

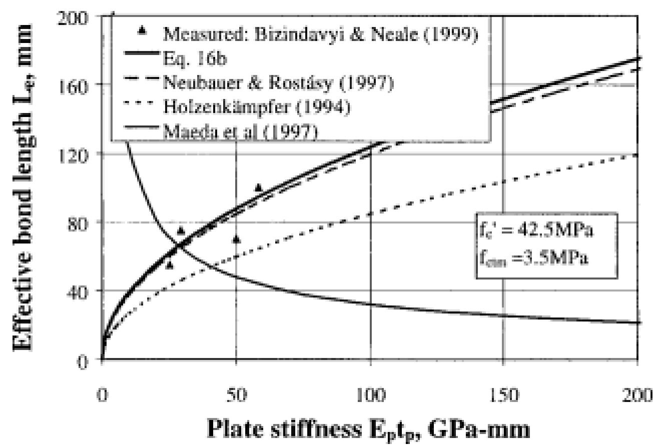

FIG. 6. Effect of Bonded Plate Stiffness on Effective Bond Length

TABLE 3. Effective Bond Length L_e (mm)

Data source	Test specimen (Table 1)	Measured	Prediction: Khalifa et al. (1998)	Prediction: Neubauer and Rostásy (1997)	Prediction: Present (16)	Present/ Measured
Bizindavyi and Neale (1999)	BN1 (GFRP)	75	65.1	64.6	66.9	0.89
Bizindavyi and Neale (1999)	BN2 (GFRP)	100	43.6	91.3	94.6	0.95
Bizindavyi and Neale (1999)	BN3 (CFRP)	55	71.3	59.7	61.9	1.13
Bizindavyi and Neale (1999)	BN4 (CFRP)	70	47.7	84.5	87.5	1.25
Täljsten (1997)	S100-40A to S800-80A (steel)	~300	11.3	260–280	275–293	0.94

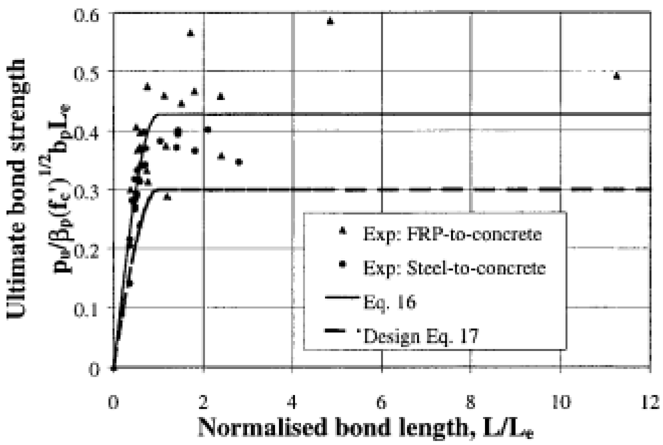

FIG. 7. Effect of Bond Length on Ultimate Bond Strength

scattered around the curve predicted by (16), statistically val-idating the important concept of the effective bond length.

Anchorage Strength Design

The coefficient in (16) may be reduced to the 95th percentile characteristic value of 0.427 × (1 — 1.64 × 0.159) = 0.315, so that it can be used for ultimate strength design to concrete. Existing test data suggest that the main failure mode is concrete failure under shear, occurring generally at a few millimeters from the concrete-to-adhesive surface. The bond strength, therefore, depends strongly on the concrete strength. In addition, the plate-to-concrete member width ratio has a significant effect. A very important aspect of bond be- havior is that there exists an effective bond length beyond which an extension of the bond length cannot increase the bond strength. This is a fundamental difference between the anchorage design of an externally bonded plate and an internal reinforcement for which a sufficiently long anchorage length can always be found, so that the full tensile strength of the reinforcement can be achieved. Thin stiff plates (e.g., carbon plates) should be used to make the best use of the tensile strength of the bonded plate.

Existing bond strength models, including empirical models, fracture mechanics models, and simple design models, have been reviewed and assessed by comparison with experimental data gathered from the literature. This enabled the identifica- tion of the deficiencies of the existing models, generally dueto the omission of one or more of the important aspects men- tioned above, such as the effective bond length limit.

Finally, a new simple design model has been developed. This new model is modified from an existing fracture me- chanics model with suitable simplifications, and captures allof the main features of anchorage behavior. Both the anchor-

$P_u = 0.315\beta_p\beta_L\sqrt{f_c'}b_pL_e$ age strength and the effective bond length can be correctly

Some studies (Swamy et al. 1986) showed that the cracking load at the loaded end is about 60% of the ultimate load. Therefore, the coefficient in (17) may be further reduced to

0.315 × 0.6 ≈ 0.2 for serviceability state design (without cracking)

predicted using this new model.

REFERENCES

In practical design, generally a designer needs to know the stress rather than the load carried by the FRP plate. Substitut- ing (16*b*) and $\sigma_p = P_u/b_pt_p$ into (16*a*) gives the stress in the bonded plate at failure

Chaallal, O., Nollet, M. J., and Perraton, D. (1998). ''Strengthening of reinforced concrete beams with externally bonded fibre-reinforced-plas-tic plates: Design guidelines for shear and flexure.'' *Can. J. Civ. Engrg.*,Ottawa, 25(4), 692–704.
Chajes, M. J., Finch, W. W. Jr., Januszka, T. F., and Thonson, T. A. Jr. (1996). ''Bond and force transfer of composite material plates bonded to concrete.'' *ACI Struct. J.*, 93(2), 295–303.
Chajes, M. J., Januszka, T. F., Merta, D. R., Thomson, T. A. Jr., and Finch, W. W. Jr. (1995). ''Shear strengthening of reinforced concrete beams using externally applied composite fabrics.'' *ACI Struct. J.*, 92(3), 295–303.
Deutsches Institut für Normung, e.V. (1991). "DIN1048, Augsgabe 6.91, Teil 2: Prüfverfahren für Beton, Festbeton in Bauwerken und Bautei- len.'' Beuth Verlag, Berlin (in German).
Ehsani, M. R., Saadatmanesh, H., and Tao, S. (1996). ''Design recom- mendations for bond of GFRP rebars to concrete.'' *J. Struct. Engrg.*, ASCE, 122(3), 247–254

FORCA tow sheets technical notes. (1994). Autocon Composites Inc., New York.
Fukuzawa, K., Numao, T., Wu, Z., Yoshizawa, H., and Mitsui, M. (1997).''Critical strain energy release rate of interface debonding between car- bon fibre sheet and mortar.'' *Non-Metallic (FRP) Reinforcement for Concrete Struct., Proc., 3rd Int. Symp.*, Japan Concrete Institute, Sap- poro, 1, 295–302.
Hiroyuki, Y., and Wu, Z. (1997). ''Analysis of debonding fracture prop- erties of CFS strengthened member subject to tension.'' *Non-Metallic (FRP) Reinforcement for Concrete Struct., Proc., 3rd Int. Symp.*, Japan Concrete Institute, Sapporo, 1, 287–294.
Holzenkämpfer, O. (1994). "Ingenieurmodelle des verbundes geklebter bewehrung für betonbauteile." Dissertation, TU Braunschweig (in German).
Horiguchi, T., and Saeki, N. (1997). ''Effect of test methods and quality of concrete on bond strength of CFRP sheet.'' *Non-Metallic (FRP) Reinforcement for Concrete Struct., Proc., 3rd Int. Symp.*, Japan Con- crete Institute, Sapporo, 1, 475–482.
Khalifa, A., Gold, W. J., Nanni, A., and Aziz, A. (1998). ''Contributionof externally bonded FRP to shear capacity of RC flexural members.'' *J. Compos. for Constr.*, ASCE, 2(4), 195–203.
Kobatake, Y., Kimura, K., and Ktsumata, H. (1993). ''A retrofitting method for reinforced concrete structures using carbon fibre.'' *Fibre- reinforced-plastic (FRP) reinforcement for concrete structures: Prop- erties and applications*, A. Nanni, ed., Elsevier Science, Amsterdam, 435–450.
MacGregor, J. G. (1988). *Reinforced concrete: Mechanics and design*, Prentice-Hall, Englewood Cliffs, N.J.
Maeda, T., Asano, Y., Sato, Y., Ueda, T., and Kakuta, Y. (1997). ''A studyon bond mechanism of carbon fiber sheet.'' *Non-Metallic (FRP) Re- inforcement for Concrete Struct., Proc., 3rd Int. Symp.*, Japan Concrete Institute, Sapporo, 1, 279–285.
Malek, A. M., Saadatmanesh, H., and Ehsani, M. R. (1998). ''Prediction of failure load of R/C beams strengthened with FRP plate due to stress

concentration at the plate end.'' *ACI Struct. J.*, 95(1), 142–152.

Neubauer, U., and Rostásy, F. S. (1997). ''Design aspects of concrete structures strengthened with externally bonded CFRP plates.'' *Proc., 7th Int. Conf. on Struct. Faults and Repairs*, ECS Publications, Edin- burgh, Scotland, 2, 109–118.

Niedermeier, R. (1996). ''Stellungnahme zur Richtlinie für das Verkleben von Betonbauteilen durch Ankleben von Stahllaschen—Entwurf März 1996.'' *Schreiben 1390 vom 30.10.1996 des Lehrstuhls für Massivbau*, Technische Universität München, Munich, Germany (in German).

Roberts, T. M. (1989). ''Approximate analysis of shear and normal stress concentrations in the adhesive layer of plated RC beams.'' *The Struct. Engr.*, London, 67(12/20), 229–233.

Tanaka, T. (1996). ''Shear resisting mechanism of reinforced concrete beams with CFS as shear reinforcement.'' Graduation thesis, Hokkaido University, Japan.

Teng, J. G., Chen, J. F., Smith, S. T., and Lam, L. (2000). *RC structures strengthened with FRP composites*, The Hong Kong Polytechnic Uni- versity, Hong Kong, China.

Triantafillou, T. C., and Plevris, N. (1992). ''Strengthening of RC beams with epoxy-bonded fibre-composite materials.'' *Mat. and Struct.*, Paris, 25, 201–211.

van Gemert, D. (1980). ''Force transfer in epoxy-bonded steel-concrete joints.'' *Int. J. Adhesion and Adhesives*, 1, 67–72.

Varastehpour, H., and Hamelin, P. (1996). ''Analysis and study of failure mechanism of RC beams strengthened with FRP plate.'' *Proc., 2nd Int. Conf. on Advanced Compos. Mat. in Bridges and Struct.*, M. El-Badry, ed., Canadian Society for Civil Engineering, Montreal, 527–537.

Volnyy, V. A., and Pantelides, C. P. (1999). ''Bond length of CFRP com- posites attached to precast concrete walls.'' *J. Compos. for Constr.*, ASCE, 3(4), 168–176.

Yuan, H., and Wu, Z. (1999). ''Interfacial fracture theory in structures strengthened with composite of continuous fiber.'' *Proc., Symp. of China and Japan: Sci. and Technol. of 21st Century*, Tokyo, Sept., 142–155.

Yuan, H., Wu, Z. S., and Yoshizawa, H. (2001). ''Theoretical solutionson interfacial stress transfer of externally bonded steel/composite lam- inates.'' *J. Struct. Mech. and Earthquake Engrg.*, Tokyo, in press.

Zhang, S., Raoof, M., and Wood, L. A. (1997). ''Prediction of peelingfailure of reinforced concrete beams with externally bonded plates.'' *Proc., Inst. of Civ. Engrs., Struct. and Build.*, London, 122, 493–496. Ziraba, Y. N., Baluch, M. H., Basunbul, A. M., Azad, A. K., Al-Sulaimani, G. J., and Sharif, I. A. (1995). ''Combined experimental-numerical ap- proach to characterization of steel-glue-concrete interface.'' *Mat. and Struct.*, Paris, 28, 518–525.